J. Eng. Technol. Sci., Vol. 54, No. 5, 2022, 220508

# Design Optimization of Propellant Grain and Nozzle Contour to Improve Performance of Solid Rocket Propulsion

**Muhammad Ihsan Abyan[1], Aang Nuryaman[1,*], Bagus Hayatul Jihad[2], Soleh Fajar Junjunan[2] & Asmiati[1]**

[1]Department of Mathematics, Faculty of Mathematics and Natural Sciences, Universitas Lampung, Jalan Soemantri Brojonegoro No. 1, Bandarlampung, Indonesia
[2]Research Centor for Rocket Technology, National Research and Innovation Agency (BRIN), Jalan Raya LAPAN No. 2, Mekarsari, Rumpin, Bogor 16350
[*]E-mail: aang.nuryaman@fmipa.unila.ac.id

**Highlights:**

- The precise configuration of the propellant grain to improve the performance of a rocket motor.
- Geometry analysis of the propellant grain configuration as the basis for solving the optimization problem of maximizing the total rocket impulse.
- The operating parameters of the optimized rocket motor increase the rocket motor's performance by 10% higher.

**Abstract** A rocket is a spacecraft, guided missile, or flying vehicle that boosted by a chemical reaction resulting from the combustion of propellant in the rocket motor. One of the essential parameters in the development of rocket motors is design optimization to improve the propulsion performance of the rocket. Increasing the propulsion performance of the rocket will increase the flight performance of the rocket, in terms of its maximum range or the altitude of the rocket trajectory. This study examined the determination of the design parameter values of a rocket motor by looking at it as an optimization problem with constraints. The problem studied was limited to the case of the second-stage rocket motor. A genetic algorithm was used to solve the resulting optimization problem of propellant grain configuration cases and a characteristic method for designing the bell nozzle. The results obtained indicated an increase in total impulse by 10% compared to the results before optimization.

**Keywords**: *dual stage; genetic algorithm; method of characteristic optimizations; nozzle; propellant grain.*

## 1 Introduction

In 2012, the Center for Rocket Technology of the National Institute of Aeronautics and Space (Pustekroket LAPAN) began developing the RX-450

Received October 27th, 2021, 1st Revision February 26th, 2022, 2nd Revision May 11th, 2022, Accepted for publication June 21st, 2022.

DOI: 10.5614/j.eng.technol.sci.2022.54.5.8

.

rocket as an experimental rocket to meet the challenge of a three-digit rocket, namely a rocket capable of reaching an altitude of 100 km. Pustekroket LAPAN tried to increase the range of the RX-450 in 2020 to reach a height of 200 km in an effort to bring Indonesian satellites into low earth orbit (LEO). Therefore, Pustekroket LAPAN developed the RX-450 design into a dual-stage rocket with two propulsion engines. The first stage is used to get sufficient thrust to lift off. The second stage is used to provide thrust after the first stage has been released from the rocket so it can reach a longer distance.

One of the most critical factors in increasing a rocket's range is improving the performance of the rocket motor, which uses solid propellant fuel, liner, igniter, and a nozzle. In solid propellant rockets, the rocket motor's performance depends on the propellant geometry and nozzle design characteristics. Grain is a solid propellant mass processed in the rocket motor [1]. The propellant material and the geometric configuration of the grain determine the performance characteristics of the motor. Most rockets have a single grain, in their rocket motor components, some rocket motors have more than one grain. A very small number of grains have segments with a different propellant composition. The grain configuration is designed to meet various requirements to obtain optimal thrust.

Researchers have carried out research related to the optimization of grain propellants. Raza & Liang [2] used a genetic algorithm, simulated annealing, and a combination of genetic and simulated annealing algorithms to optimize dual thrust propellant. The results showed that the genetic algorithm could produce the most significant increase in thrust, while the genetic algorithm hybrid method and simulated annealing could reduce the computation time. Then Al-Farizi, *et al*. [3] optimized the RX-450 star grain propellant configuration before developing it into a dual-stage rocket using the real-code genetic algorithm. The genetic algorithm method is widely used in grain propellant optimization because it can be applied to functions with discontinuities and detect the global optimum.

In addition to optimizing the grain configuration, the nozzle design is also essential. Most current LAPAN rockets use conical nozzles. Shekhar, *et al*. [4] compared the performance between a conical nozzle and a bell nozzle. A bell nozzle has two advantages: it can minimize the weight of the nozzle itself and maximize the rocket motor's performance. Khan, *et al*. [5] concluded that the characteristic method is a perfect for use in designing a bell nozzle. Therefore, in this study, we determined the design of the star grain and bell nozzle related to the parameters of the physical properties of the rocket in the second stage of the RX-450 using solid propellant.

Designing the star grain was done to obtain the grain configuration parameter values necessary to produce maximum thrust, which is indicated by the burning area. One of the concepts used to obtain the combustion area of a rocket motor is a grain burn back analysis based on geometric theory. The problem of determining the parameter values according to the burn back analysis results was considered as an optimization problem to maximize the total rocket impulse and to minimize the weight of the propulsion design, which was solved using a genetic algorithm. Meanwhile, the bell nozzle design was constructed using the characteristics method. Studies on genetic algorithms and their applications can be found in [6] and [7].

## 2 Mathematical Modelling

In this article, we consider the optimization problems to improve the performance of the RX-450 rocket motor by using star grain propellant. Star grain is a form of propellant that is widely used because it has the advantage of being easy to manufacture. In addition, in terms of performance, star grain has the advantage of having a sizeable initial combustion area, resulting in a sizeable initial thrust. A thing to consider when choosing a star grain is the neutrality of the combustion chamber pressure profile. Davenas [8] states that star grain has a large sliver of about 5%. Star grain has a radial combustion direction.

The star geometry configuration has unique properties compared to other propellants. Its nature is that the thrust versus time profile can be progressive, neutral, or regressive. Seven independent variables need to be known to design the star grain: namely outer radian spoke radian ($R_p$), number of spokes ($N$), fillet ($f$), inner fillet ($r$), star angle ($\xi$), and separation angle ($\eta$). Based on these variables, a burning back analysis is used to obtain the grain's combustion area. A further explanation of burn back analysis and its applications can be found in [9-15].

### 2.1 Burn Back Analysis

In the star grain configuration, there is a change in the angle in the first possible third phase ($\gamma$ and $\delta$) and the second possible third phase ($\alpha$), which can be defined as follows:

$$\gamma = \pi - \cos^{-1}\left(\frac{R_o^2 - R_p^2 - (f+y)^2}{-2R_p(f+y)}\right)$$

$$\delta = \sin^{-1}\left(\frac{y+f}{R_o}\sin(\pi-\gamma)\right)$$

.

$$\alpha = \cos^{-1}\left(\frac{R_p \sin(\xi)}{y+f}\right)$$

In the first phase of star grain combustion, there is the constraint that the configuration magnification ($y$) cannot exceed $r$ so that the condition $y < r$ applies. Thus, we have that the burning area $A_b$ and the port area $A_p$ in each phase are:

Phase 1:

$$S1 = (R_p + f + y)\left(\frac{\pi}{N} - \xi\right)$$

$$S2 = (f + y)\left(\frac{\pi}{2} - \eta + \xi\right)$$

$$S3 = \left(\frac{R_p \sin(\xi)}{\sin(\eta)}\right) - \left(\frac{(r-y)\sin\left(\frac{\pi}{2} - \eta\right)}{\sin(\eta)}\right)$$

$$S4 = (r - y)\left(\frac{\pi}{2} - \eta\right)$$

Thus, the burning area in phase 1 is:

$$A_b = 2N(S1 + S2 + S3 + S4)L$$

The port area of the star grain for phase 1 is given by:

$$A_p = 2N(A1 + A2 + A3 + A4)$$

where

$$A1 = \frac{1}{2}\left(R_p + f + y\right)^2\left(\frac{\pi}{N} - \xi\right) \quad (1)$$

$$A2 = \frac{1}{2}(f + y)^2\left(\frac{\pi}{2} - \eta + \xi\right) \quad (2)$$

$$A3 = \frac{1}{2}R_p \sin(\xi)\left(R_p \cos(\xi) + R_p \sin(\xi)\tan(\eta)\right) - \frac{1}{2}S3^2\tan(\eta) \quad (3)$$

$$A4 = \left(\frac{1}{2}\left(\frac{(r-y)\sin\left(\frac{\pi}{2} - \eta\right)}{\sin(\eta)}\right)(r - y)\right) - \left(\frac{1}{2}(r - y)^2\left(\frac{\pi}{2} - \eta\right)\right)$$

The condition for phase 1 to end is when $r = 0$ or $S4 = 0$. It will continue to the second phase with a new limit, namely $y \geq r$, as illustrated in Figure 1.

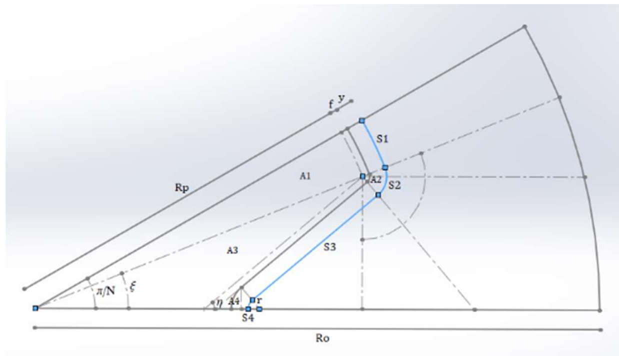


**Figure 1** Phase 1 of star grain.

For phase 2, based on Figure 2, we have that the formulas for $S1$ and $S2$ are the same as in phase 1. The formula for S3 is given by:

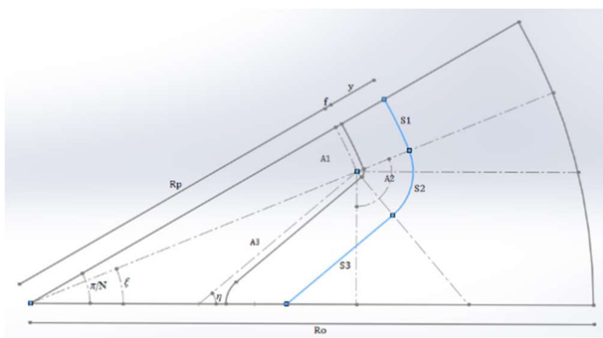


**Figure 2** Phase 2 of star grain.

$$S3 = \left(\frac{R_p \sin(\xi)}{\sin(\eta)}\right) - (f + y) \cot(\eta)$$

Thus, the burning area in phase 2 is:

$$A_b = 2N(S1 + S2 + S3)L$$

And the port area is given by:

$$A_p = 2N(A1 + A2 + A3)$$

with $A1$, $A2$ and $A3$ respectively, given by Eq. (1)-(3). There are two possible conditions for phase 2 to end. The first is when $S1 = 0$ or $y = R_o - R_p - f$ and the second is when $S3 = 0$ or $y = \sqrt{\left(R_p \sin\xi \tan\eta\right)^2 + \left(R_p \sin\xi\right)^2} - f$.

.

For phase 3, when S1 burns out first ($S1 = 0$), as shown in Figure 3, we obtain the burning area as:

$$A_b = 2N(S2 + S3)L$$

with

$$S2 = (f + y)\left(\frac{\pi}{2} + \xi - \eta - \gamma\right)$$

$$S3 = \left(\frac{R_p \sin(\xi)}{\sin(\eta)}\right) - (f + y)\cot(\eta)$$

As for the port area, we have $A_p = 2N(A1 + A2 + A3)$ with

$$A1 = \frac{1}{2} {R_o}^2 \left(\frac{\pi}{N} - \xi + \delta\right) - \frac{1}{2} R_o R_p \sin(\delta)$$

$$A2 = \frac{1}{2}(f + y)^2 \left(\frac{\pi}{2} + \xi - \eta - \gamma\right)$$

$$A3 = \frac{1}{2} R_p \sin(\xi)\left(R_p \cos(\xi) + R_p \sin(\xi)\tan(\eta)\right) - \frac{1}{2} S3^2 \tan(\eta)$$

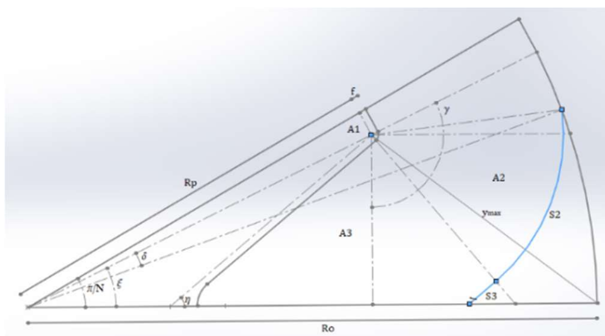


**Figure 3** The first possibility of phase 2 of star grain.

The first possible condition that ends phase 3 is S3 = 0, i.e., when $y = \sqrt{\left(R_p \sin\xi \tan\eta\right)^2 + \left(R_p \sin\xi\right)^2} - f$.

On the other hand, if S3 runs out first ($S3 = 0$), as shown in Figure 4, we have that the burning area is:

$$A_b = 2N(S1 + S2)L$$

with

$$S1 = (R_p + f + y)\left(\frac{\pi}{N} - \xi\right)$$

$$S2 = (f + y)\left(\frac{\pi}{2} - \alpha + \xi\right)$$

and the port area, we have $A_p = 2N(A1 + A2 + A3)$ with

$$A1 = \frac{1}{2}\left(R_p + f + y\right)^2\left(\frac{\pi}{N} - \xi\right)$$

$$A2 = \frac{1}{2}(f + y)^2\left(\frac{\pi}{2} - \alpha + \xi\right)$$

$$A3 = \frac{1}{2}\, R_p \sin(\xi)\left(R_p \cos(\xi) + (y + f)\sin(\alpha)\right)$$

The second possible condition that ends phase 3 is S1 = 0, i.e., when $y = R_o - R_p - f$.

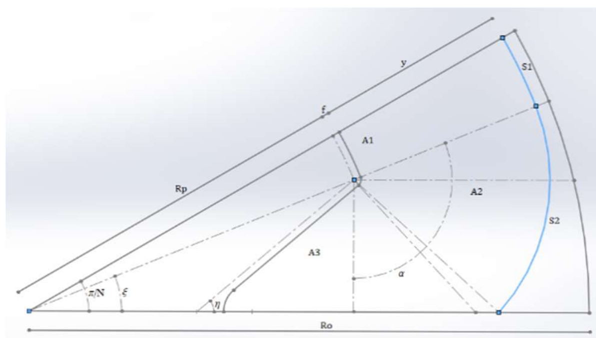


**Figure 4** The second possibility of phase 2 of star grain.

Only sliver or propellant combustion remains in the fourth phase, which does not provide enough energy to add thrust to the rocket. Thus, the fourth phase or sliver is not used to determine the total impulse in the mass balance calculation. For this phase (see Figure 5), we have that the burning area is:

$$A_b = 2N\left((f + y)\left(\frac{\pi}{2} + \xi - \alpha - \gamma\right)\right)L$$

And the port is given by $Ap = 2N(A1 + A2 + A3)$ with

$$A1 = \frac{1}{2}\, {R_o}^2\left(\frac{\pi}{N} - \xi + \delta\right) - \frac{1}{2}\, R_o\, R_p \sin(\delta)$$

$$A2 = \frac{1}{2}(f + y)^2\left(\frac{\pi}{2} + \xi - \alpha - \gamma\right)$$

$$A3 = \frac{1}{2}\, R_p \sin(\xi)\left(R_p \cos(\xi) + (y + f)\sin(\alpha)\right)$$

.

The condition that ends phase 4 is when all of the propellants have burned out, i.e., when $y = \sqrt{\left(R_o - R_p \cos \xi\right)^2 + \left(R_p \sin \xi\right)^2} - f$.

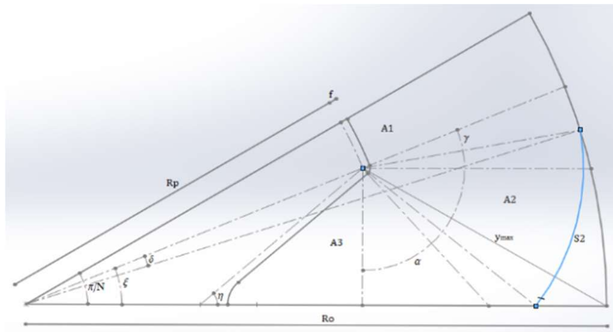


**Figure 5** Phase 5 of star grain.

## 2.2 Model Formulation

The objective function used in this study is a function that maximizes the value of the total impulse. The constraints used on the rocket motor used to consist of a design constraint and a performance constraint. The design constraint was obtained from the independent variables forming a star grain configuration with seven spokes. The performance constraint was obtained from the initial performance of the rocket motor before the rocket motor was optimized. The objective function and constraints of our problem were:

$$F(x) = \min(-I_t)$$

Subject to:

$$100 \le R_p \le 160,$$
$$0.5 \le f \le 10,$$
$$5 \le r \le 20,$$
$$29 \le \eta \le 38,$$
$$15 \le \xi \le 24,$$
$$\max(P_c) < 70,$$
$$(\pi {R_o}^2 L - Ap_1 L)\rho < 840,$$
$$\max(F) - \min(F) < 0.20 \max(F),$$
$$\frac{\sum_{i=1}^{n} C_{F(i)}\, P_c(i)\, A_t}{n} > 95210,$$

where, $I_t$ denotes the total impulse. For the calculation of the combustion pressure ($P_c$) this study used the mass-balance equation:

$$P_c = \left(\frac{\rho_p A_b a c^*}{A_t}\right)^{\frac{1}{1-n}}$$

The mass balance equation uses the assumption that the rate of addition of a gas in the combustion chamber is the same as the rate of mass passing through the nozzle, which is only accurate for obtaining pressure at a steady-state, namely in phases 1, 2, and 3. Then from the combustion pressure, the thrust profile against time can be determined with the formula

$$F = C_F \, P_c \, A_t \, \eta_N$$

The total impulse is defined as the integral of the thrust over the combustion time.

$$I_t = \int_0^{t_b} F \, dt$$

# 3 Design Results

## 3.1 Solid Propellant Grain Design

In this study, the genetic algorithm used a population consisting of 5,000 random individuals in the hope of obtaining a diverse initial population and meeting optimization constraints. After the initial population is set, the next step is to evaluate the fitness function of each individual in the population. In some cases, after the fitness function is evaluated, several individuals show undefined results (NaN). Therefore, proper individual selection is used to overcome this problem by converting the undefined result to zero. Thus, undefined results do not interfere with the sorting process.

The individuals are then ordered from the smallest to the largest fitness function. Each individual who meets the performance constraint is multiplied by $-1$ so that when sorted, it will rise to first place. Furthermore, individuals who meet the conditions are entered into the crossover process while others are eliminated. In the crossover process, the best individuals are always paired with other individuals in the hope of getting offspring that have a better fitness function than their parents. Then, a new population is obtained, namely the initial population and the population resulting from crossover.

After the new population has been obtained, the next step is to re-calculate the fitness function of the new population, and select the appropriate individuals as before and then do the sorting. This is again done to prepare the population to enter the mutation stage. Mutations are always carried out on 10% of the population, which produces the worst fitness function.

.

From the genetic algorithm's optimization process, the results started to be constant from the 30th iteration at a total impulse of 1,730,697 Ns. This means that based on the initial population obtained from 5,000 randomly selected genes, the gene that produced the maximum total impulse was obtained (see Figure 6).

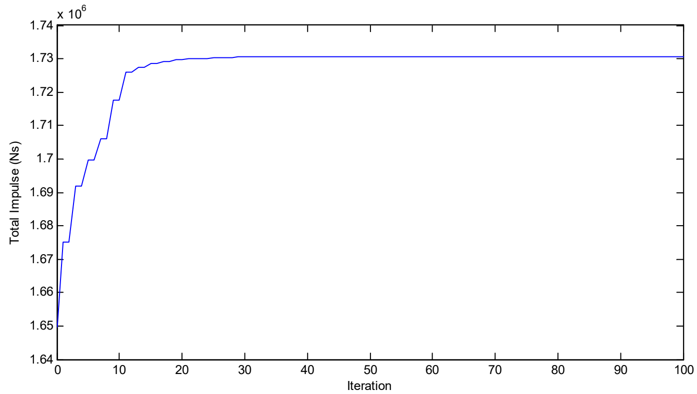


**Figure 6** The best individual optimization graph for each iteration.

After crossover and mutation, the input parameters of the optimization results were obtained, as shown in Table 1.

**Table 1** Input parameters for grain optimization results.

| Parameter | Notation | Values |
|---|---|---|
| Number of spokes | $N$ | 7 |
| Outer radian | $R_o$ | 216 |
| Spoke radian | $R_p$ | 122.47084 |
| Fillet | $f$ | 0.9517001 |
| Internal fillet | $r$ | 15.743604 |
| Separation angle | $\eta$ | 29.886584 |
| Star angle | $\xi$ | 23.463264 |

Based on the parameters obtained from the optimization results of the grain design, the optimized grain could be constructed, as shown in Figure 7.

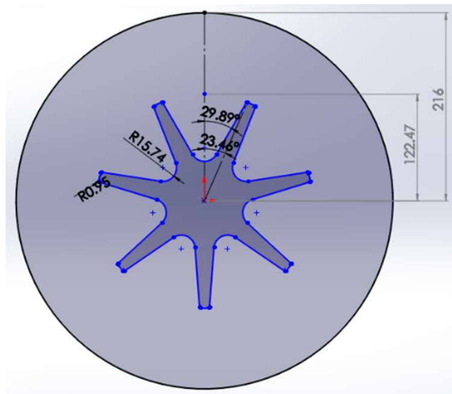


**Figure 7** Star grain design.

From the grain shape obtained, we could determine the thickness profile of the propellant (web) to the combustion area and get a profile, as shown in Figure 8. The combustion area produced by the optimized grain was 50,599 cm$^2$ with a range of 48,413 cm$^2$ to 53,792 cm$^2$.

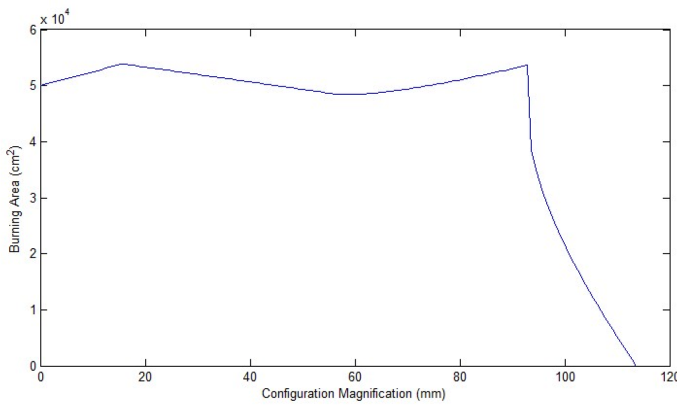


**Figure 8** Plot of web vs burning area.

## 3.2 Bell Nozzle Design

The nozzle serves to convert heat energy from combustion into kinetic energy. The most crucial thing in the nozzle design is determining the radius of the nozzle throat. The radius of the nozzle throat evaluates the area of the nozzle throat. The size of the nozzle throat area affects the combustion pressure. The smaller the nozzle throat area, the greater the combustion pressure. The radius

.

of the nozzle throat was determined to be 75 mm, and the type of nozzle used was a bell nozzle.

The contours of the bell nozzle divergent section found in this study were obtained using the characteristics method proposed by Khan, *et al.* in [5]. The characteristics method gave a Mach number and a base angle of the divergent section ($\theta_{max}$) of 2.96 M and 31.21°, respectively. The centerline point and contour of the divergent section obtained using the characteristics method can be seen in Figures 9 and 10. From the resulting nozzle contour graph, the parameters for the nozzle design could be determined, as shown in Table 2.

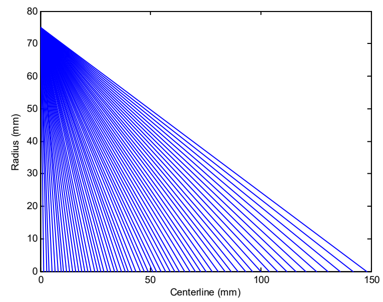


**Figure 9** Centerline point

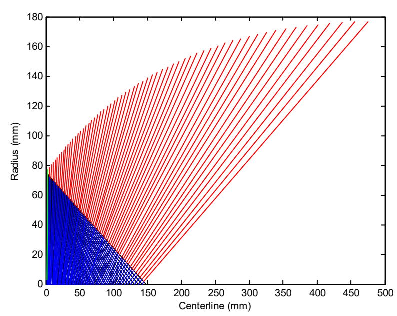


**Figure 10** Divergent section.

**Table 2** Nozzle parameters using the characteristics method.

| Nozzle Parameters | Notations | Values |
|---|---|---|
| Throat nozzle radius | $r_t$ | 75 mm |
| Exit nozzle radius | $r_e$ | 176.53 mm |
| Nozzle length | $L_n$ | 659.64 mm |
| Maximal divergent angle | $\theta_{max}$ | 31.21 deg |
| Convergent angle | | 45 deg |
| Inlet nozzle fillet radius | | 110 mm |
| Throat nozzle fillet radius | | 80 mm |

Based on the parameters obtained, the design of the bell nozzle was developed, as shown in Figure 11.

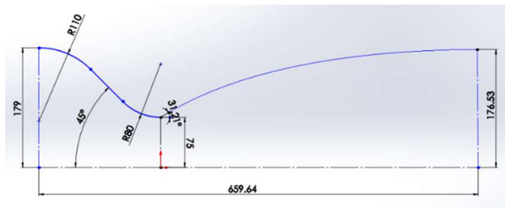


**Figure 11** Bell nozzle design.

### 3.3 Propulsion Performance

The total impulse displayed in this study only considered the thrust at steady-state. It ignored the fourth phase because it is not very accurate, and the fourth phase only contains the remaining propellant from combustion (sliver), which does not provide significant thrust for the rocket. The propellant's characteristics that were used to determine the propulsion performance are shown in Table 3.

**Table 3** Propellant's characteristics.

| Parameters | Values |
|---|---|
| Molecular weight | 23.39 kg/kg·mole |
| Density | 0.0016243 kg/cm$^3$ |
| Gas characteristic speed | 149088 cm/s |
| Combustion rate coefficient | 0.027 inc/s |
| Specific heat ratio | 1.1887 |
| Combustion index | 0.318 |

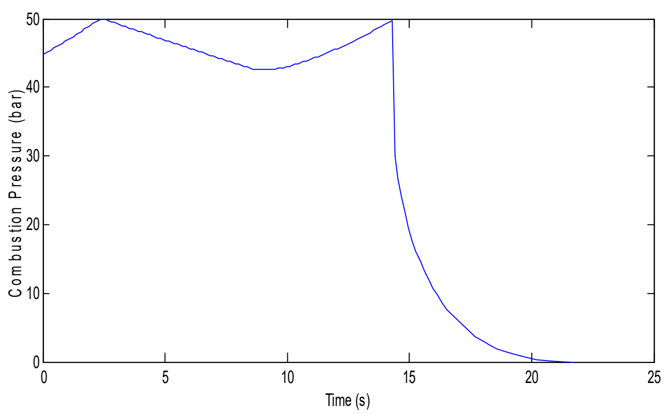


**Figure 12** Plot of combustion time vs pressure.

.

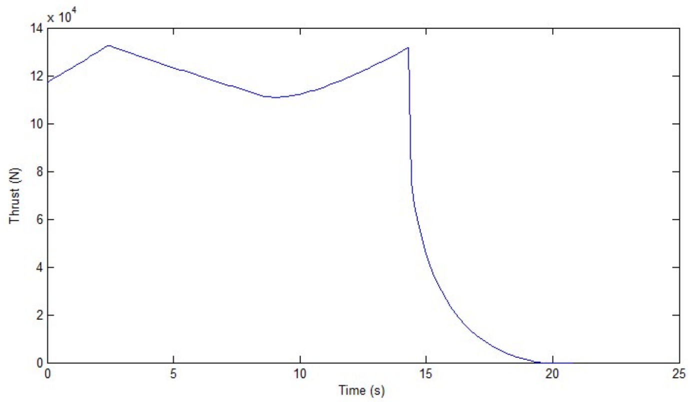


**Figure 13** Plot of time vs thrust.

Based on Figure 12, the average combustion pressure generated by the optimized grain was 45.7 bar, within a range of 42.5 to 49.9 bar. Figure 13 shows that the average thrust generated by the grain optimization result was 120,156 N with a range of 110,922.3 N to 132,327.6 N.

This study's optimization of the grain configuration used an 80% neutrality constraint, i.e., the maximum thrust value minus the minimum thrust value must be less than 20% of the maximum thrust value. In the grain optimization, the results obtained a thrust neutrality percentage of 84%. Table 4 compares the propulsion design performance before and after optimization.

**Table 4** Propulsion performance.

| | Notation | Before Optimization | After Optimization |
|---|---|---|---|
| Total impulse | $I_t$ | 1,570,490 N·s | 1,730,697 N·s |
| Average thrust | $F$ | 95,210 N | 120,156 N |
| Weight | $W$ | 840 Kg | 715 Kg |
| Burning time | $t_b$ | 16.5 s | 14.3 s |

The total impulse increased by 10% from the initial total impulse, and the average thrust generated increased by 26%. As expected, the weight decreased by 15% with a faster burning time.

## 4 Conclusions

This research provides information about developing an experimental rocket design, type RX 450 at Pustekroket LAPAN into a two-stage rocket with two combustion engines. Based on preliminary data on the physical properties of the rocket at Pustekroket LAPAN, the rocket's performance was improved by developing the design of the two main components of the rocket, namely the grain propellant and the nozzle.

In this study, we considered the configuration of star grain propellant because this type of propellant has several advantages. For the nozzle, the bell nozzle type was tried out as an alternative because most of the current rockets at Pustektroket LAPAN use a conical nozzle type.

The aim of developing the star grain propellant configuration was to maximize the rocket's thrust, represented by the total impulse of the rocket until it reaches an altitude of 200 kilometers or more. Determination of the parameter values for the star grain propellant configuration was done by solving the optimization problem of maximizing the total rocket impulse, which was then solved using a genetic algorithm. The bell nozzle design was developed using characteristics method with a predetermined throat nozzle radius and convergent angle. The characteristics method resulted in optimal values for the exit nozzle, nozzle length, and maximum diverging angle. The results obtained based on the grain configuration and design parameters of the optimized nozzle showed an increase in the total impulse of 10% compared to before optimization.

## Acknowledgments

The author would like to thank Pustekroket LAPAN for providing the data needed in this study and the Institute for Research and Community Service (LPPM) Universitas Lampung, which has funded this research with contract number 1647/UN26.21/PN/2021. Also, the authors would like to thank the reviewers for their invaluable suggestions and corrections.

## References

[1] Sutton, G.P. & Biblarz, O., *Rocket Propulsion Elements*, 8th Edition, John Wiley & Sons, Inc., Hoboken, 2010.

[2] Raza, M.A. & Liang, W., Design *and Optimization of 3D Wagon Wheel Grain for Dual Thrust Solid Rocket Motor*, Propellants, Explosives, Pyrotechnics. **38**(1), pp. 67-74, 2013.

[3] Al Farizi, M.F., Bura, R.O., Junjunan, S.F. & Jihad, B.H., *Grain Propellant Optimization Using Real Code Genetic Algorithm (RCGA),* Journal of Physics: Conference Series. **1005**(1), pp. 1-12, 2018.

[4] Shekhar, A.C., Sarma, S.B.S. & Govind, R.LR., *CFD Analysis on Conical and Bell Nozzle*, International Journal of Engineering of Technology, Management and Applied Science, **5**(6), pp. 952-955, 2017.

.


[5] Khan, M.A., Sardiwal, S.K., Sharath, M.V.S. & Chowdary, D.H., *Design of a Supersonic Nozzle using Method of Characteristics*, International Journal of Engineering Research & Technology, **2**(11), pp. 19-24, 2013.

[6] Eshelman, L.J. & Schaffer, J.D., *Real-Coded Genetic Algorithms and Interval-Schemata*, Foundations of Genetic Algorithms, **2**, pp. 187-202. 1993.

[7] Michalewicz, Z., *Genetic Algorithm + Data Structure = Evolution Programs,* 3rd Edition. Springer-Verlag Berlin Heidelberg, New York, 1996.

[8] Davenas, A., *Solid Rocket Propulsion Technology*. Pergamon Press, Oxford, 1993.

[9] Püskülcü, G. & Ulas, A., *3-D Grain Burnback Analysis of Solid Propellant Rocket Motors: Part 1 – Ballistic Motor Tests*, Aerospace Science and Technology, **12**(8), pp. 579-584, 2008.

[10] Püskülcü, G. & Ulas, A., *3-D Grain Burnback Analysis of Solid Propellant Rocket Motors: Part 2 – Modeling and Simulations*, Aerospace Science and Technology, **12**(8), pp. 579-584, 2008.

[11] Tola, C. & Nikbay, M., *Internal Ballistic Modeling of a Solid Rocket Motor by Analytical Burnback Analysis*, Journal of Spacecraft and Rockets, **56**(2), pp. 498-516, 2018. DOI: 10.2514/1.A34065.

[12] Oh, S.H., Lee, S.B., Kim, Y.C., Cha, S.W., Kim, K.R., Kim, D.M. & Roh, T.S., *Study on Solid Propellant Grain Burn-back Analysis Applying Face Offsetting Method*, Journal of the Korean Society of Propulsion Engineers. **23**(4), pp. 81-91, 2019. DOI: 10.6108/kspe.2019.23.4.081.

[13] Reddy, K.O. & Pandey, K.M., *Burnback Analysis of 3-D Star Grain Solid Propellant*, International Journal of Advanced Trends in Computer Science and Engineering, **2**(1), pp. 215-223, 2013.

[14] Mehdi, G.M., & Mehdi, M.S., *Using Marching Cube Algorithm for 3D Grain Burn-Back Analysis in Solid Rocket Motors Based on Level Set Method*, Modares Mechanical Engineering, **14**(15), pp. 85-95, 2015.

[15] Sohn, J., Jang, J., Oh, S. & Roh, T., *Study on Solid Propellant Grain Burn-back Analysis Using Analytical Method*, Journal of the Korean Society of Propulsion Engineers, The Korean Society of Propulsion Engineers, **18**(3), pp. 40-47, June 2014.